

HLIC: Harmonizing Optimization Metrics in Learned Image Compression by Reinforcement Learning

Baocheng Sun Meng Gu Dailan He Tongda Xu Yan Wang* Hongwei Qin
SenseTime Research

{sunbaocheng, gumeng, hedailan, xutongda, wangyan1, qinhongwei}@sensetime.com

Abstract

Learned image compression is making good progress in recent years. Peak signal-to-noise ratio (PSNR) and multi-scale structural similarity (MS-SSIM) are the two most popular evaluation metrics. As different metrics only reflect certain aspects of human perception, works in this field normally optimize two models using PSNR and MS-SSIM as loss function separately, which is suboptimal and makes it difficult to select the model with best visual quality or overall performance. Towards solving this problem, we propose to Harmonize optimization metrics in Learned Image Compression (HLIC) using online loss function adaptation by reinforcement learning. By doing so, we are able to leverage the advantages of both PSNR and MS-SSIM, achieving better visual quality and higher VMAF score. To our knowledge, our work is the first to explore automatic loss function adaptation for harmonizing optimization metrics in low level vision tasks like learned image compression.

1. Introduction

With the growth of information technology, image capturing and sharing have become ubiquitous. The purpose of image compression is to reduce storage and transmission cost.

The basic idea of image compression is to reduce image signal redundancies by considering spatial correlations, statistical representations and human vision sensitivity. Traditional image compression methods, such as JPEG [13], JPEG2000 [31], BPG [6] and the intra coding of VVC/VTM [1, 12], all rely on hand-crafted modules. They incorporate intra prediction, discrete cosine transform/wavelet transform, quantization and entropy coder such as Huffman coder or content adaptive binary arithmetic coder (CABAC) [27] to remove such redundancies.

In recent years, deep learning and computer vision meth-

ods are introduced to create novel and powerful image compression techniques [32, 36, 5, 22, 9, 8]. They utilize modern neural networks to obtain compact image representations, which can be subsequently quantized and compressed by standard entropy coding algorithms. Bit rate and image quality are constrained by loss function. Various entropy models [36, 4, 28, 5, 8] are designed as differentiable proxy to bit rate, proved to be very effective. The assessment of image quality is still an open problem. In image and video coding tasks, peak signal-to-noise ratio (PSNR) and multi-scale structural similarity (MS-SSIM) [39] are two most common metrics. Both of them are differentiable and can be adopted as the distortion part in loss function. The trade-off between bit rate and distortion can be controlled by adjusting the weight between entropy loss and distortion loss.

It is known that fitting to different optimization metrics can cause different visual artifacts. And the choice of distortion loss is difficult [5, 29]. Works in the field of learned image compression tend to train two models optimizing PSNR and MS-SSIM separately. Models optimized for PSNR often have unsatisfactory performance on MS-SSIM, and vice versa [5, 30, 8]. A linear hybrid of mean squared error (MSE, the only non-constant part in PSNR) and MS-SSIM has been used as perceptual loss in previous leading solutions to learned image compression challenge (CLIC) [42, 43]. DSSIM proposed by [15] is designed as L_1 loss weighted by SSIM, which performs better than L_1 loss regarding PSNR, SSIM and MS-SSIM. Although these studies try to harmonize PSNR and MS-SSIM by hand-crafted loss function, deeper analysis and more automatic method are still lacking. For example, to what extent we can harmonize PSNR and MS-SSIM in one model, how to control the harmonization result conveniently, and how to do metric harmonization automatically or dynamically in the whole training process.

In this paper, we aim to harmonize the optimization of PSNR and MS-SSIM in learned image compression by dynamically adapting the loss function using reinforcement learning (RL). Our contributions can be summarized as follows: 1) Our work is the first to investigate automatic loss

*Corresponding author. This work is done when Baocheng Sun and Meng Gu are interns at SenseTime Research.

function adaptation for metric harmonization in low level vision tasks like learned image compression. 2) We propose an effective framework for controlling metric harmonization, which achieves improved and controllable tradeoff between PSNR and MS-SSIM. 3) We demonstrate the improvement brought by harmonious optimization on the famous perceptual metric VMAF [24] and human perceptual quality, bringing new insight into image quality optimization for low level vision tasks.

2. Related Work

2.1. Learned Image Compression

A number of powerful learned image compression methods have emerged with the rapid development of deep learning [3]. Ballé *et al.* [4] propose an autoencoder based structure to perform nonlinear transform coding of images. The output of encoder is quantized and viewed as latent code to be compressed by lossless entropy coders. Later, [5] extends this model by utilizing hyperprior to capture the interdependency of latent representation, leading to a much more powerful entropy model. Inspired by PixelCNN [37], the hyperprior model is extended by adding an autoregressive module to further exploit the probabilistic structure of the latent code [30]. Cheng *et al.* [8] propose to use more powerful neural network architectures and use Gaussian Mixture Model (GMM) for entropy modelling, which is the first work comparable with the intra coding of Versatile Video Coding (VVC) [12] regarding PSNR.

As stated in the introduction, works in this field normally train two separate models optimizing PSNR and MS-SSIM respectively. A few studies investigate the harmonization of different metrics by hand-crafted loss function [42, 43, 15]. However, as mentioned above, there are still problems to be investigated.

2.2. Visual Quality Optimization

PSNR is the de facto standard for traditional codec comparison [24]. However, this pixel-based difference measurement correlates poorly with human perception [11, 23]. MS-SSIM is another popular and differentiable metric widely used in image compression. While not directly related to human perception, it obtains better subjective ratings than PSNR. Images obtained by optimizing PSNR have clearer structural information, and images obtained by optimizing MS-SSIM retain more texture [5, 19].

In recent years, VMAF [24] uses Support Vector Machine to fuse a number of elementary metrics, such as VIF [35] and DLM [23]. It achieves good subjective rating results and has become an industry standard for video coding. Unfortunately, It is not differentiable and cannot be used directly for optimizing learned image compression. ProxIQa [7] proposes a proxy network to mimic VMAF,

which is used as loss function for learned image compression, leading to 20% bitrate reduction to MSE-optimized baseline under the same VMAF value.

VGG based loss has been used in diverse tasks as perceptual constraint [14, 18]. However, it does not perform well in learned image compression due to unpleasant artifacts [29].

2.3. Loss Function Search/Adaptation

Loss function search is an AutoML technology and becomes popular recently. By dynamically optimizing the parameters of loss function’s distribution using REINFORCE algorithm [40], AM-LFS [20] surpasses hand-crafted loss functions in classification, face recognition and person ReID. Wang *et al.* [38] further improves this method for face recognition by redesigning the search space based on deeper analysis of margin-based softmax losses. Very recently, Ada-Segment [41] extends the idea of AM-LFS to perform multi-loss adaptation for panoptic segmentation. Auto Seg-Loss [21] proposes to search for parameterized metric-specific surrogate loss in semantic segmentation. CSE-Autoloss [25] proposes to discover novel loss functions for object detection automatically by searching combinations of primitive mathematical operations with evolutionary algorithm.

Existing works mainly focus on high-level vision tasks including classification, object detection, face recognition, person ReID and segmentation. However, those high-level tasks have a large difference with image compression, a typical low-level task. In high-level tasks, mis-alignment between loss function and evaluation metrics degrades the performance, leaving relatively larger room for improvement by loss function search or adaptation methods. In image compression, popular evaluation metrics including PSNR and MS-SSIM can be used as loss function. So it is much more difficulty to achieve performance improvement regrading these two metrics. In addition, in low level vision tasks no single evaluation metric or known combinations can well represent the ultimate goal of optimizing human visual perception, which brings additional complexity.

3. Proposed Method

3.1. Differentiable Rate-Distortion Optimization

We formulate image compression as a differentiable rate-distortion (RD) optimization problem following previous works [5, 30, 8]. Figure 1 shows a typical model architecture. First, the input image x is fed into a neural encoder g_a and transformed into latent representation y . Then we quantize it to get the code \hat{y} to be compressed. Since the rounding operator has zero gradients everywhere, additive uniform noise $q \sim \mathcal{U}(-\frac{1}{2}, \frac{1}{2})$ is introduced as a relaxation, generating $\tilde{y} = y + q$ which approximates \hat{y} during train-

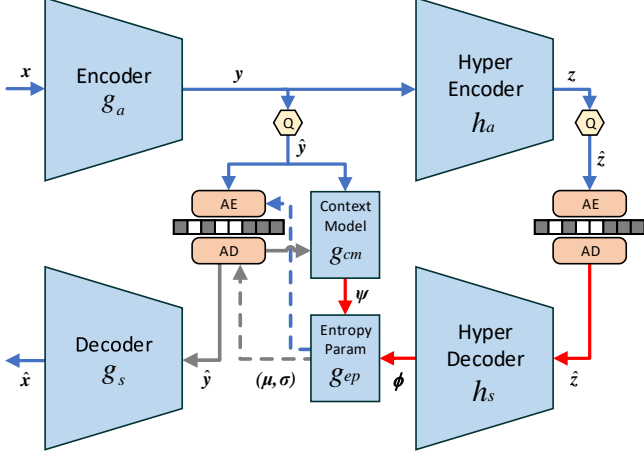


Figure 1. Diagram of autoregressive compression models [30, 8]. The blue and gray arrows denote encoding and decoding data flow respectively while the red ones are shared by both encoding and decoding process.

ing [4, 5]. For simplicity, below we use \hat{y} to denote both \hat{y} and \tilde{y} . Side-information z is further extracted from y by a hyper encoder h_a . Then it is quantized as \hat{z} and get compressed into bitstream accompanied with \hat{y} . The same relaxation is applied to generate \tilde{z} in training. During decoding, side-information \hat{z} is decompressed from the bitstream first and transformed by the hyper decoder h_s to predict the distribution $p_{\hat{y}|\hat{z}}$. After that, \hat{y} can be decompressed and finally the output image \hat{x} can be reconstructed from \hat{y} by transform g_s .

The distribution $p_{\hat{y}|\hat{z}}$ can be modelled as:

$$p_{\hat{y}|\hat{z}}(\hat{y}) = \prod_i \left(\mathcal{N}(\mu_i, \sigma_i^2) * \mathcal{U}\left(-\frac{1}{2}, \frac{1}{2}\right)(\hat{y}_i) \right) \quad (1)$$

where i indicates the element id in \hat{y} and μ_i is set to 0 in [5]. The probability of \hat{z} is modeled using a non-parametric fully factorized density model proposed in [4]. The probability model for \hat{y} and \hat{z} is used in the compression and decompression process of entropy coding. Also, they are part of the loss function to enable differentiable RD trade-off, where the bit rate is approximated using entropy:

$$\begin{aligned} L &= R + D \\ &= \mathbb{E}_{x \sim p_x} [-\log_2 p_{\hat{y}|\hat{z}}(\hat{y}|\hat{z}) - \log_2 p_{\hat{z}}(\hat{z})] \\ &\quad + \lambda \cdot \mathbb{E}_{x \sim p_x} [d(x, \hat{x})] \end{aligned} \quad (2)$$

where distortion weight λ controls the RD trade-off. As introduced in section 1, distortion term $d(x, \hat{x})$ is usually MSE or $1 - \text{MS-SSIM}$.

Minnen *et al.* [30] propose an autoregressive method to

better estimate $p_{\hat{y}|\hat{z}}$, which can be formulated as:

$$\begin{aligned} \psi_i &= g_{cm}(\hat{y}_{<i}) \\ \phi &= h_s(\hat{z}) \\ \mu_i, \sigma_i &= g_{ep}(\phi, \psi_i) \end{aligned} \quad (3)$$

$$p_{\hat{y}|\hat{z}} = \prod_i \left(\mathcal{N}(\mu_i, \sigma_i^2) * \mathcal{U}\left(-\frac{1}{2}, \frac{1}{2}\right) \right) (\hat{y}_i)$$

where $\hat{y}_{<i}$ means the context of \hat{y}_i (*i.e.* some accessible neighbours), g_{cm} and g_{ep} are also transforms using neural networks. Cheng *et al.* [8] extends this method by using Gaussian Mixture Model to estimate $p_{\hat{y}|\hat{z}}$:

$$p_{\hat{y}|\hat{z}} = \prod_i \left\{ \sum_{0 < k < K} \pi_i^{(k)} \left[\mathcal{N}(\mu_i^{(k)}, \sigma_i^{2(k)}) * \mathcal{U}\left(-\frac{1}{2}, \frac{1}{2}\right) \right] (\hat{y}_i) \right\} \quad (4)$$

where K groups of entropy parameters $(\pi^{(k)}, \mu^{(k)}, \sigma^{(k)})$ are generated by g_{ep} .

3.2. Metric Harmonization by Loss Function Adaptation

3.2.1 Adaptation Space

Based on analysis above, the adaptation space of distortion loss D can be formulated as:

$$D = \lambda_{\text{MSE}} \cdot \text{MSE} + \lambda_{\text{MS-SSIM}} \cdot (1 - \text{MS-SSIM}) \quad (5)$$

where MSE and $1 - \text{MS-SSIM}$ are the loss function for optimization metric PSNR and MS-SSIM respectively. As λ_{MSE} and $\lambda_{\text{MS-SSIM}}$ are always positive, we use the trick of reparameterization:

$$\begin{aligned} \lambda_{\text{MSE}} &= e^{\lambda'_{\text{MSE}}} \\ \lambda_{\text{MS-SSIM}} &= e^{\lambda'_{\text{MS-SSIM}}} \end{aligned} \quad (6)$$

where λ'_{MSE} and $\lambda'_{\text{MS-SSIM}}$ are the parameters to be adapted online (as a sequence of values) throughout the training process. We observe that in eq. 2 the change in distortion weight λ and the final bit rate forms a logarithm relationship. So in eq. 6 changes in λ'_{MSE} and $\lambda'_{\text{MS-SSIM}}$ are almost proportional to changes in bit rate. Such mapping makes it easier for RL to converge on desirable λ'_{MSE} and $\lambda'_{\text{MS-SSIM}}$ corresponding to different target bit rates.

3.2.2 Reward Design

Reward design is the key of controllable metric harmonization and improvement. Our reward consists of three parts and depends on two baseline RD curves optimized for PSNR and MS-SSIM separately. Denote the model parameterized by θ as \mathcal{M}_θ and the validation set as S_v . The reward

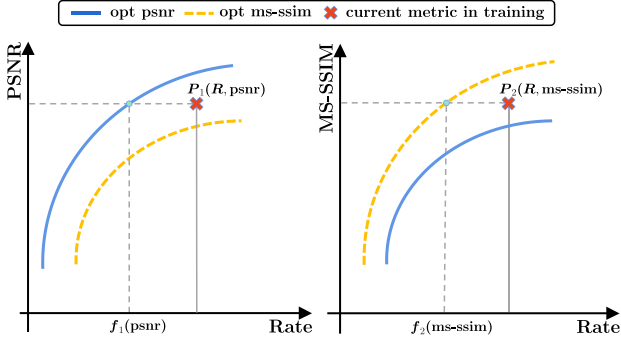


Figure 2. Mapping functions in the reward design. Blue and yellow RD curves denote baselines trained using MSE and MS-SSIM as distortion loss respectively. Red mark means current (R, psnr) and $(R, \text{ms-ssim})$.

can be formulated as a function of \mathcal{M}_θ and \mathcal{S}_v :

$$\begin{aligned}
\mathcal{R} &= r(\mathcal{M}_\theta; \mathcal{S}_v) \\
&= \mathcal{W}_1\left(\frac{R - R_{target}}{R_{target}}\right) \\
&+ \mathcal{W}_2\left(\frac{R - f_1(\text{psnr})}{f_1(\text{psnr})}\right) \\
&+ \mathcal{W}_3\left(\frac{R - f_2(\text{ms-ssim})}{f_2(\text{ms-ssim})}\right)
\end{aligned} \tag{7}$$

where R is current bits per pixel (bpp). The function f_1 and f_2 represent the mapping from current metric value (denoted as lower-case psnr and ms-ssim in eq. 7 and Figure 2) to corresponding bpp value in the baseline RD curves. The first part encourages the bit rate to be the target one, the second and the third parts encourage the model to converge to the best RD tradeoff regarding PSNR and MS-SSIM respectively. For different purposes, the three targets can be weighted and reshaped using different functions \mathcal{W}_i .

We design two types of experiments to demonstrate that our method can control and improve metric harmonization. For the First type, \mathcal{W}_i can be expressed as:

$$\begin{aligned}
\mathcal{W}_1(x) &= w_1 x^2 \\
\mathcal{W}_2(x) &= 0 \\
\mathcal{W}_3(x) &= w_3 x
\end{aligned} \tag{8}$$

We set $w_1 = 25, w_3 = 10$, which encourages the model to focus on optimizing MS-SSIM (section 5.1). For the second type, \mathcal{W}_i can be expressed as:

$$\mathcal{W}_i(x) = w_i x^2 \quad (i = 1, 2, 3) \tag{9}$$

where w_i is used to control the priority between PSNR and MS-SSIM (section 5.2). To optimize PSNR while giving attention to MS-SSIM, we set $w_1 = 25, w_2 = 100, w_3 = 1$. To optimize MS-SSIM while giving attention to PSNR, we set $w_1 = 25, w_2 = 1, w_3 = 100$.

3.2.3 Optimization

Algorithm 1 PPO-based Loss Function Adaptation

Input: Initialized model $\mathcal{M}_{\theta_0^*}$, epoch T , the number of samples B , trajectory length N

Output: optimal model $\mathcal{M}_{\theta_T^*}$

$r_0^i, \mathbf{o}_1^i \leftarrow \text{EVAL}(\mathcal{M}_{\theta_0^*}; \mathcal{S}_v), i \in \{1, \dots, B\}$

for $t \leftarrow 1$ to T **do**

for $i \leftarrow 1$ to B **do** \triangleright train B models separately

 Sample distortion weights $\lambda_t^i \sim \pi_{\omega_p}(\cdot | \mathbf{o}_t^i)$

$\mathcal{M}_{\theta_t^i} \leftarrow \text{TRAIN}(\mathcal{M}_{\theta_{t-1}^i}; \mathcal{S}_t, \lambda_t^i)$

$r_t^i, \mathbf{o}_{t+1}^i \leftarrow \text{EVAL}(\mathcal{M}_{\theta_t^i}; \mathcal{S}_v)$

end for

if $t \bmod N = 0$ **then**

 Update $\omega_p \leftarrow \text{argmax}_{\omega_p} \mathbb{E}_{\pi_{\omega_p}}[\sum_{i,t} r_t^i]$

 index $\leftarrow \text{argmax}_{j \in [1, B]} r_t^j$

$\mathcal{M}_{\theta_t^*} \leftarrow \mathcal{M}_{\theta_t^{\text{index}}}$

end if

end for

return $\mathcal{M}_{\theta_T^*}$

We denote the training set as \mathcal{S}_t , the validation set as \mathcal{S}_v , and the image as \mathbf{x} . Here we are adapting hyper-parameters $\lambda = (\lambda_{\text{MSE}}^i, \lambda_{\text{MS-SSIM}}^i)$ defined in eq. 6 online for a specific model \mathcal{M}_θ . Before the t^{th} epoch of training, an observation \mathbf{o}_t is made. \mathbf{o}_t contains validation results from $(t - 1)^{\text{th}}$ epoch including MS-SSIM, PSNR, bpp of $\hat{\mathbf{y}}$, bpp of $\hat{\mathbf{z}}$, gradient loss and total variation [26]. The online adapting policy $\pi_{\omega_p}(\lambda | \mathbf{o}_t)$ is a distribution over λ parameterized by ω_p . Our target of loss function adaptation is to maximize the expectation of reward $r(\mathcal{M}_\theta; \mathcal{S}_v)$ in eq. 7 and the weight θ is obtained by minimizing the online adapted RD loss modified from eq. 2 and eq. 5:

$$\pi^* = \text{argmax}_{\{\pi(\cdot | \mathbf{o})\}} \mathbb{E}_{\lambda \sim \pi(\cdot | \mathbf{o})} \left[\sum_t r_t(\mathcal{M}_{\theta^*}(\lambda); \mathcal{S}_v) \right]$$

s.t.

$$\begin{aligned}
\theta^*(\lambda) &= \text{argmin}_{\{\theta\}} \frac{1}{\#\mathcal{S}_t} \sum_{\mathbf{x} \in \mathcal{S}_t} (R + \lambda_{\text{MSE}} \cdot \text{MSE} \\
&\quad + \lambda_{\text{MS-SSIM}} \cdot (1 - \text{MS-SSIM}))
\end{aligned} \tag{10}$$

where $\#\mathcal{S}_t$ denotes the size of training set. To solve this bi-level optimization problem, [20] adopts REINFORCE [40]. However, REINFORCE suffers from unstable training due to high variance.

We tackle this problem with Proximal Policy Optimization (PPO) [34]. After observation \mathbf{o}_t is made, we sample distortion weights λ_t from policy $\pi_{\omega_p}(\cdot | \mathbf{o}_t)$ for t^{th} epoch. Our policy is normal distribution with $\mu_\lambda, \sigma_\lambda$ controlled by

a multi-layer perceptron (MLP):

$$\begin{aligned} \lambda_t &\sim \pi_{\omega_p}(\cdot|\mathbf{o}_t) \\ \pi_{\omega_p}(\cdot|\mathbf{o}_t) &= \mathcal{N}(\boldsymbol{\mu}_\lambda, \boldsymbol{\sigma}_\lambda^2) \\ \text{with } \boldsymbol{\mu}_\lambda, \boldsymbol{\sigma}_\lambda &= \mathcal{MLP}(\mathbf{o}_t) \end{aligned} \quad (11)$$

After training B models with distortion weight λ_t for t^{th} epoch, we validate these models to obtain reward $r_t = r(\mathcal{M}_{\theta_t}; \mathcal{S}_v)$ and the next observation \mathbf{o}_{t+1} . To reduce the variance of the gradient estimation, we utilize critic [17] and generalized advantage estimation [33] to compute advantage \hat{A}_t .

Every N epoch of training, we generate B trajectories of length N . Then, we optimize the parameters ω_p of policy π_{ω_p} by minimizing surrogate loss L^{CLIP} :

$$\begin{aligned} L^{\text{CLIP}}(\omega_p) &= \hat{\mathbb{E}}_t \left[\min \left(f_t(\omega_p) \hat{A}_t, \right. \right. \\ &\quad \left. \left. \text{CLIP}(f_t(\omega_p), 1 - \epsilon, 1 + \epsilon) \hat{A}_t \right) \right] \quad (12) \\ \text{with } f_t(\omega_p) &= \frac{\pi_{\omega_p}(\lambda_t|\mathbf{o}_t)}{\pi_{\omega_{p_t}}(\lambda_t|\mathbf{o}_t)} \end{aligned}$$

where the clipping ratio ϵ is 0.2 and f_t is the important sampling factor. Furthermore, we broadcast the model $\mathcal{M}_{\theta_t^*}$ with the highest reward $r(\mathcal{M}_{\theta_t^*}; \mathcal{S}_v)$ to initialize the B models in the next epoch.

The full pipeline is presented in Algorithm 1.

4. Implementation Details

Training Details: We investigate our proposed metric harmonization framework based on two representative learned image compression methods: Ballé2018 [5] and Cheng2020 [8]. We use same network architectures following original paper. We selected 8000 largest pictures from the Imagenet dataset [10] as the training set \mathcal{S}_t . According to previous works [4, 5], we add uniform random noise to each picture, and then perform down-sampling. During the training process, the picture is cropped into samples with the size of 256×256 . All models are trained for 2000 epochs (*i.e.* 1M steps) with a batch-size of 16 and use a constant learning rate of 1×10^{-4} if not specified. To optimize the policy, we use the Adam optimizer with a learning rate of $\eta_{\theta_p} = 0.0003$, $\beta_1 = 0.9$ and $\beta_2 = 0.999$. The number of samples B is set to 8. More detailed description is given in the appendix.

Evaluation: We use Kodak dataset [16] as our validation set \mathcal{S}_v and Tecnick dataset [2] as our test set.

Traditional Codecs: We also compare our methods with VTM, BPG and JPEG.

5. Experiments

5.1. Effectiveness and Ablation Study

In order to show the effectiveness of our purposed method, we compare it with the most common training method for learned image compression, where only MS-SSIM is used as loss function (marked as Ballé2018[MS-SSIM](reproduction) in Figure 3 and Figure 4). We use the reward defined in eq. 8, where we only encourage MS-SSIM. We find that the RD performance not only improves on PSNR, but also slightly improves on MS-SSIM. Using the same reward, we also test PPO with a trajectory length of 1 and REINFORCE for comparisons, but they are unable to achieve the result of PPO with a trajectory length of 10. Previous works [5, 30, 8] show that if only one metric is optimized, the test result of the other one will perform very poor. Our experimental results show that if MSE is utilized skillfully in the loss function, MS-SSIM can be further improved slightly, and at the same time PSNR can be improved apparently compared with only optimizing MS-SSIM baseline. This indicates that the optimization of PSNR and MS-SSIM can be harmonized to some extent. We take the adapted loss function at the last iteration of HLIC and use it as a fixed loss function to retrain a new model from scratch (marked with retrain in Figure 3 and Figure 4), which performs apparently worse than our HLIC method, indicating that the proposed online loss adaptation process benefits the harmonization of PSNR and MS-SSIM.

5.2. Controllable Metric Harmonization

We compare our proposed method with the result of hand-crafted hybrid loss similar to [42, 43], which can also harmonize the optimization. For manually optimizing MS-SSIM preferentially while considering MSE (marked as Manual-id[MS-SSIM] in Figure 5), the hand-crafted distortion weight λ is selected as:

$$\begin{aligned} \lambda_{\text{MS-SSIM}} &= \frac{120}{4^j}, \lambda_{\text{MSE}} = \frac{0.0128 \times 2^i}{4^j} \\ \lambda_{\text{bpp}} &= 1, (i = 0, \dots, 5; j = 0, \dots, 3) \end{aligned} \quad (13)$$

For optimizing MSE preferentially while considering MS-SSIM (marked as Manual-id[MSE] in Figure 5), the distortion weight λ is selected as:

$$\begin{aligned} \lambda_{\text{MS-SSIM}} &= \frac{3 \times 2^i}{4^j}, \lambda_{\text{MSE}} = \frac{0.08}{4^j} \\ \lambda_{\text{bpp}} &= 1, (i = 0, \dots, 5; j = 0, \dots, 3) \end{aligned} \quad (14)$$

where i controls the tradeoff between PSNR and MS-SSIM, j corresponds to different bit rates.

The preference in HLIC is controlled according to eq. 9, which is designed to optimize one metric preferentially

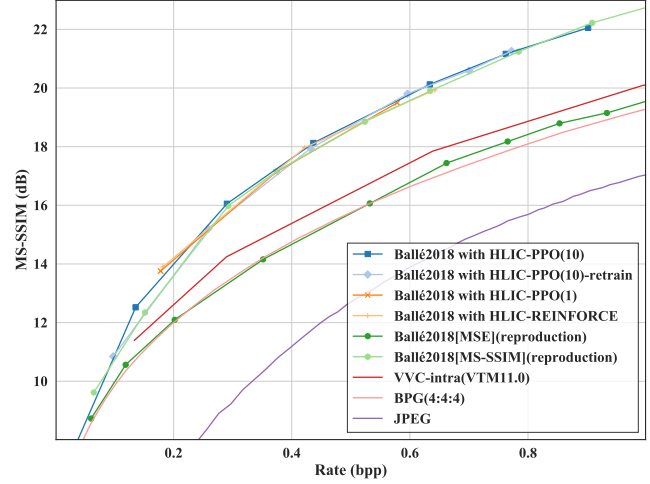
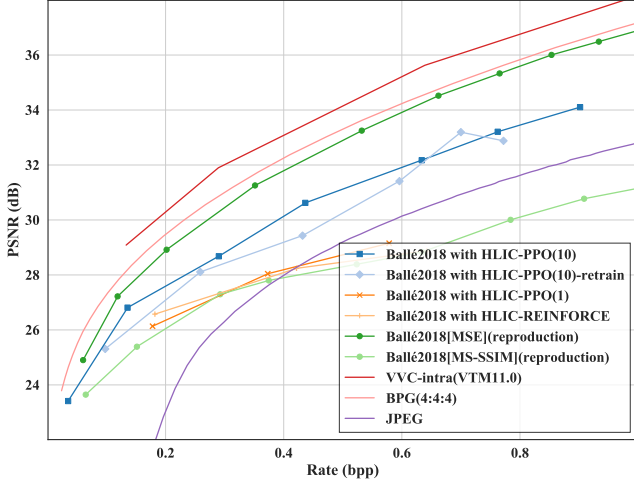


Figure 3. Ablation Study On Kodak Dataset.

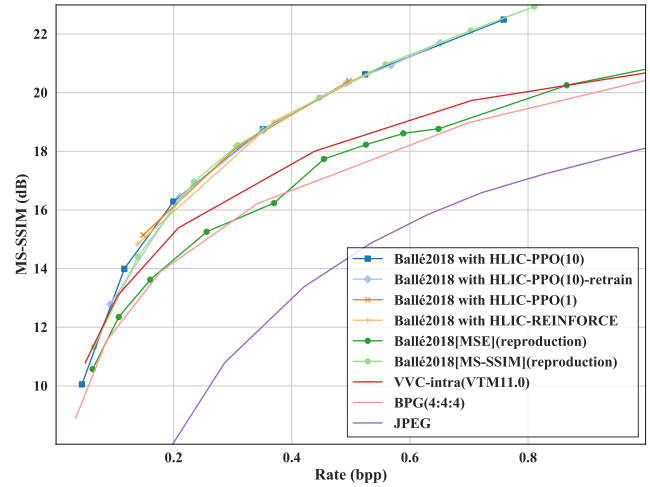
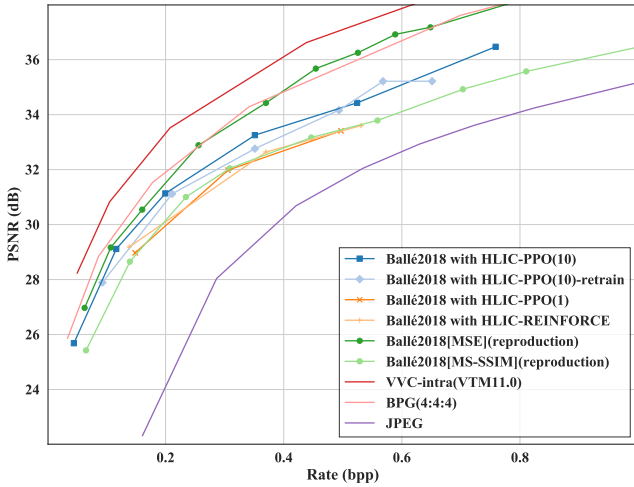


Figure 4. Ablation Study On Tecnick Dataset.

while giving attention to the other metric. HLIC[MSE] emphasizes the second term in eq. 7. HLIC[MS-SSIM] emphasizes the third term. RAL denotes using the reward as loss function directly instead of using reinforcement learning, as it is actually differentiable. Compared with hand-crafted harmonized loss function, the preferred balance point can be found by our HLIC more conveniently as we do not have to try different λ combinations like that in eq. 13 and eq. 14. RAL does not perform well and the training is not stable, showing the necessity of applying reinforcement learning. We also compare HLIC with DSSIM designed in [15] and achieve better performance overall. Similar controllable and harmonized RD performance by our HLIC on Cheng2020 [8] is shown in Figure 6.

5.3. Qualitative Results

Our method alleviates image quality problems in baseline models which optimize MSE and MS-SSIM separately. We visualize some reconstructed images from the baseline models and proposed HLIC models obtained in section 5.2.

The first two rows in Figure 7 show the reconstructed images of *kodim14* in Kodak dataset, with approximately 0.2 bpp and a compression ratio of 120:1. Although the bpp of Ballé2018[MS-SSIM] is higher and maintains reasonable texture in the water, serious color shift is produced and the text is blurred. Ballé2018[MSE] significantly reduces textures. Our two HLIC models keep reasonable textures without causing color shift.

The last two rows in Figure 7 show the reconstructed images of *kodim20*, with approximately 0.1 bpp and a compression ratio of 240:1. Ballé2018[MS-SSIM] leads to artifacts and blur in the text on the plane while

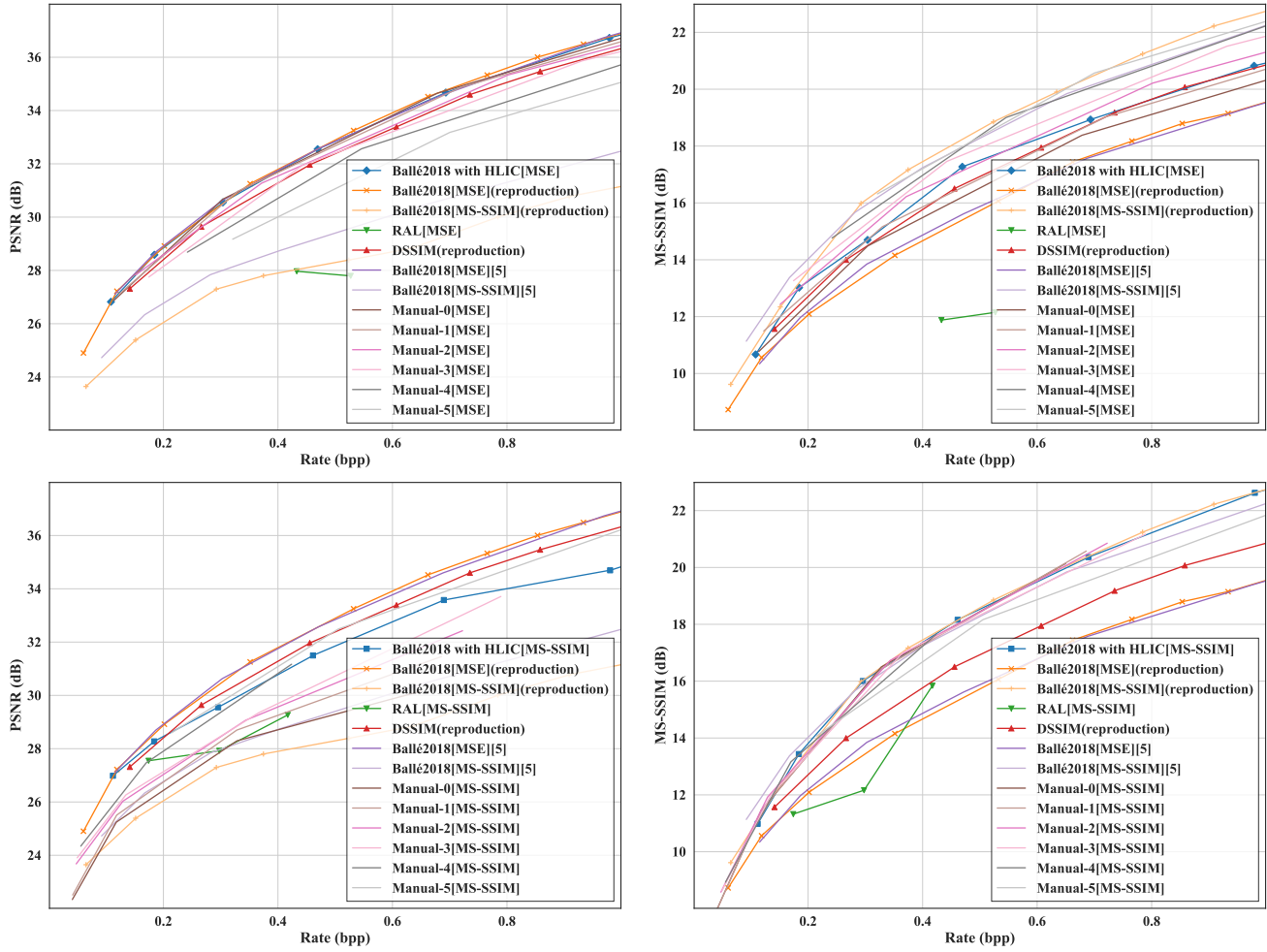


Figure 5. RD comparison with several hand-crafted loss functions on Ballé2018 [5].

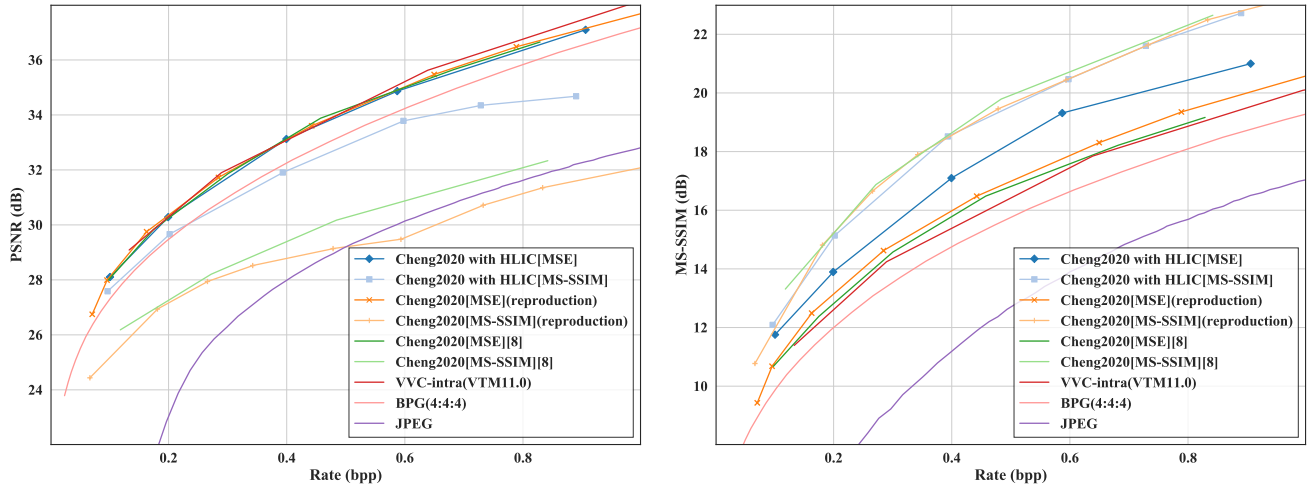


Figure 6. Harmonized RD curves evaluated on Cheng2020 [8].

Ballé2018[MSE] overly smooths the grass. Our two HLIC models perform better. We also draw VMAF with respect to

bpp in Figure 8, and our HLIC results significantly improve the VMAF compared with Ballé2018[MS-SSIM].

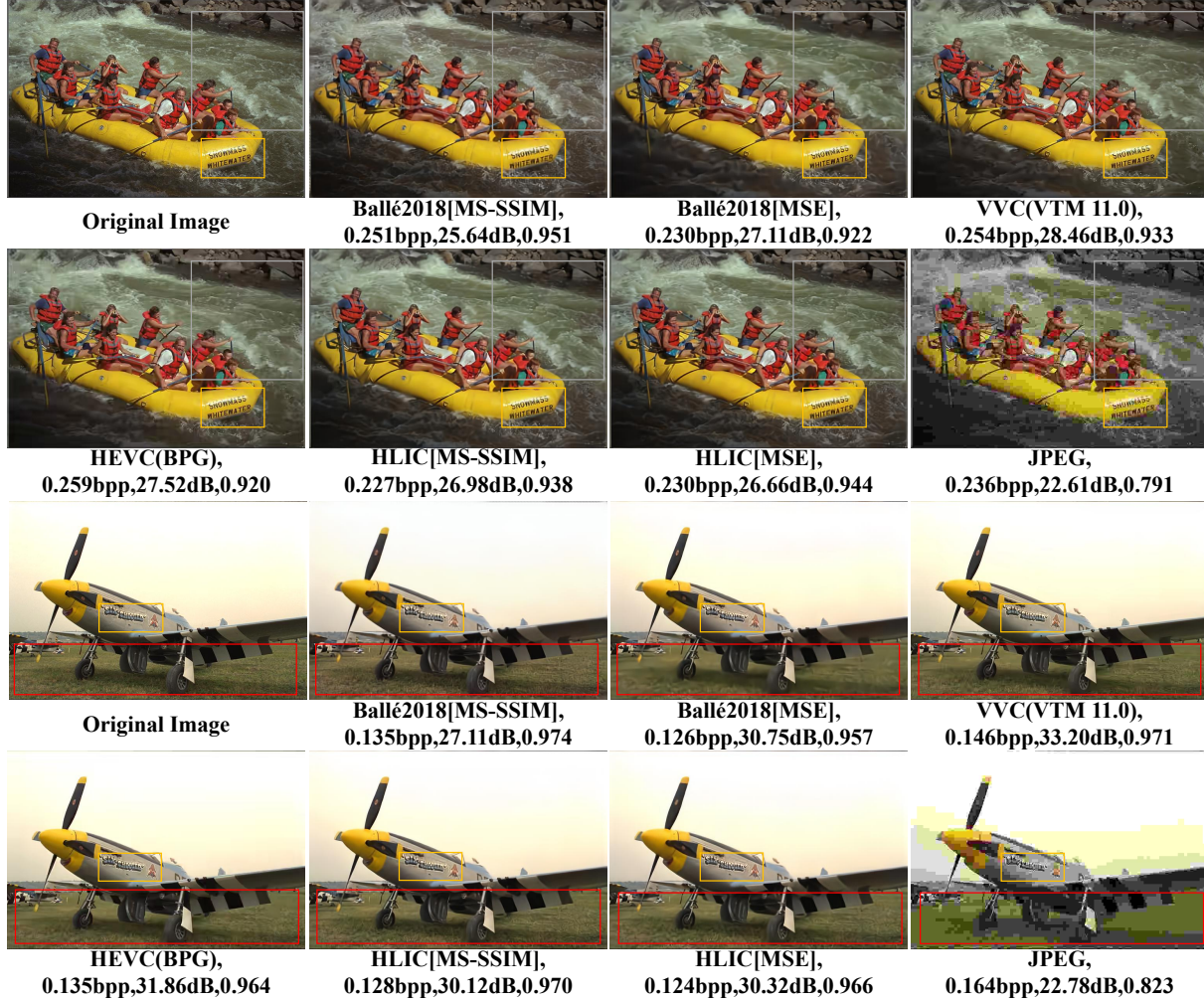


Figure 7. Visualization of reconstructed images *kodim14* and *kodim20* from Kodak dataset (better zoomed in and viewed in color).

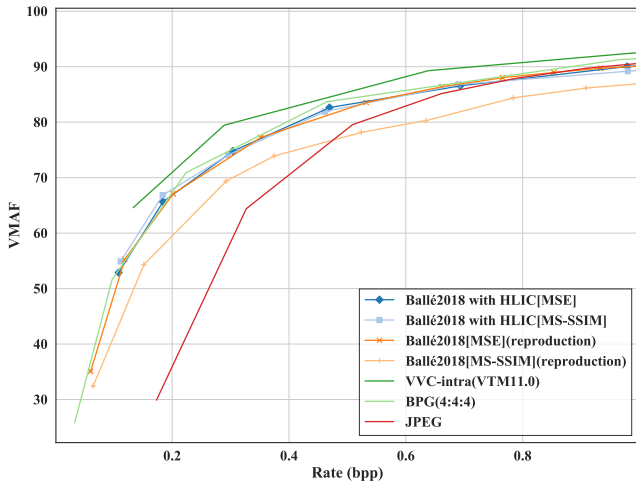


Figure 8. VMAF of the reconstructed images from our proposed methods.

6. Discussion

We propose to Harmonize optimization metrics in Learned Image Compression (HLIC) by an automatic method of online loss function adaptation. Results show the improvement in evaluation metrics as well as visual quality.

Note that although we try to harmonize PSNR and MS-SSIM in learned image compression by proposing HLIC, there still exists metric preference inevitably. As demonstrated in section 5.2, we cannot achieve best PSNR and best MS-SSIM in one model simultaneously. It is an interesting future direction to investigate more representative optimization metrics and to what extent they can be harmonized by HLIC-like methods with elaborate adaptation space.

While we only demonstrate the effectiveness of harmonizing optimization metrics for learned image compression, it can be extended to various low-level vision tasks where manually designed loss functions often do not correlate well with human perception.

References

- [1] Versatile video coding reference software version 11.0 (vtm-11.0). https://vcgit.hhi.fraunhofer.de/jvet/VVCSoftware_VTM/-/tags/VTM-11.0, 2020. **1**
- [2] Nicola Asuni and Andrea Giachetti. Testimages: a large-scale archive for testing visual devices and basic image processing algorithms. In *STAG*, pages 63–70, 2014. **5**
- [3] Johannes Ballé, Philip A Chou, David Minnen, Saurabh Singh, Nick Johnston, Eirikur Agustsson, Sung Jin Hwang, and George Toderici. Nonlinear transform coding. *arXiv preprint arXiv:2007.03034*, 2020. **2**
- [4] Johannes Ballé, Valero Laparra, and Eero P Simoncelli. End-to-end optimized image compression. In *Int. Conf. on Learning Representations*, 2017. **1, 2, 3, 5**
- [5] Johannes Ballé, David Minnen, Saurabh Singh, Sung Jin Hwang, and Nick Johnston. Variational image compression with a scale hyperprior. In *Int. Conf. on Learning Representations*, 2018. **1, 2, 3, 5, 7**
- [6] Fabrice Bellard. Bpg image format. URL <https://bellard.org/bpg>, 2015. **1**
- [7] Li-Heng Chen, Christos G Bampis, Zhi Li, Andrey Norkin, and Alan C Bovik. Proxiqa: A proxy approach to perceptual optimization of learned image compression. *IEEE Transactions on Image Processing*, 30:360–373, 2020. **2**
- [8] Zhengxue Cheng, Heming Sun, Masaru Takeuchi, and Jiro Katto. Learned image compression with discretized gaussian mixture likelihoods and attention modules. In *Proceedings of the IEEE/CVF Conference on Computer Vision and Pattern Recognition (CVPR)*, June 2020. **1, 2, 3, 5, 6, 7**
- [9] Yoojin Choi, Mostafa El-Khamy, and Jungwon Lee. Variable rate deep image compression with a conditional autoencoder. In *Proceedings of the IEEE International Conference on Computer Vision*, pages 3146–3154, 2019. **1**
- [10] Jia Deng, Wei Dong, Richard Socher, Li-Jia Li, Kai Li, and Li Fei-Fei. Imagenet: A large-scale hierarchical image database. In *2009 IEEE conference on computer vision and pattern recognition*, pages 248–255. Ieee, 2009. **5**
- [11] Bernd Girod. What’s wrong with mean-squared error? *Digital images and human vision*, pages 207–220, 1993. **2**
- [12] Information technology — Coded representation of immersive media — Part 3: Versatile video coding. Standard, International Organization for Standardization, Geneva, CH, Feb. 2020. **1, 2**
- [13] ITU. Information technology - digital compression and coding of continuous - tone still images - requirements and guidelines. *CCITT, Recommendation*, 1992. **1**
- [14] Justin Johnson, Alexandre Alahi, and Li Fei-Fei. Perceptual losses for real-time style transfer and super-resolution. In *European conference on computer vision*, pages 694–711. Springer, 2016. **2**
- [15] Nick Johnston, Damien Vincent, David Minnen, Michele Covell, Saurabh Singh, Troy Chinen, Sung Jin Hwang, Joel Shor, and George Toderici. Improved lossy image compression with priming and spatially adaptive bit rates for recurrent networks. In *Proceedings of the IEEE Conference on Computer Vision and Pattern Recognition*, pages 4385–4393, 2018. **1, 2, 6**
- [16] Eastman Kodak. Kodak lossless true color image suite (photocd pcd0992), 1993. **5**
- [17] Vijay R Konda and John N Tsitsiklis. Actor-critic algorithms. In *Advances in neural information processing systems*, pages 1008–1014. Citeseer, 2000. **5**
- [18] Christian Ledig, Lucas Theis, Ferenc Huszár, Jose Caballero, Andrew Cunningham, Alejandro Acosta, Andrew Aitken, Alykhan Tejani, Johannes Totz, Zehan Wang, et al. Photo-realistic single image super-resolution using a generative adversarial network. In *Proceedings of the IEEE conference on computer vision and pattern recognition*, pages 4681–4690, 2017. **2**
- [19] Jooyoung Lee, Donghyun Kim, Younhee Kim, Hyoungjin Kwon, Jongho Kim, and Taejin Lee. A training method for image compression networks to improve perceptual quality of reconstructions. In *Proceedings of the IEEE/CVF Conference on Computer Vision and Pattern Recognition Workshops*, pages 144–145, 2020. **2**
- [20] Chuming Li, Xin Yuan, Chen Lin, Minghao Guo, Wei Wu, Junjie Yan, and Wanli Ouyang. AM-LFS: automl for loss function search. In *2019 IEEE/CVF International Conference on Computer Vision, ICCV 2019, Seoul, Korea (South), October 27 - November 2, 2019*, pages 8409–8418. IEEE, 2019. **2, 4**
- [21] Hao Li, Chenxin Tao, Xizhou Zhu, Xiaogang Wang, Gao Huang, and Jifeng Dai. Auto seg-loss: Searching metric surrogates for semantic segmentation. *arXiv preprint arXiv:2010.07930*, 2020. **2**
- [22] Mu Li, Wangmeng Zuo, Shuhang Gu, Debin Zhao, and David Zhang. Learning convolutional networks for content-weighted image compression. In *Proceedings of the IEEE Conference on Computer Vision and Pattern Recognition*, pages 3214–3223, 2018. **1**
- [23] Songnan Li, Fan Zhang, Lin Ma, and King Ngi Ngan. Image quality assessment by separately evaluating detail losses and additive impairments. *IEEE Transactions on Multimedia*, 13(5):935–949, 2011. **2**
- [24] Zhi Li, Christos Bampis, Julie Novak, Anne Aaron, Kyle Swanson, Anush Moorthy, and Jan De Cock. Vmaf: The journey continues, Oct 2018. **2**
- [25] Peidong Liu, Gengwei Zhang, Bochao Wang, Hang Xu, Xiaodan Liang, Yong Jiang, and Zhenguo Li. Loss function discovery for object detection via convergence-simulation driven search. In *International Conference on Learning Representations*, 2021. **2**
- [26] Aravindh Mahendran and Andrea Vedaldi. Understanding deep image representations by inverting them. In *Proceedings of the IEEE conference on computer vision and pattern recognition*, pages 5188–5196, 2015. **4**
- [27] Detlev Marpe, Heiko Schwarz, and Thomas Wiegand. Context-based adaptive binary arithmetic coding in the h. 264/avc video compression standard. *IEEE Transactions on circuits and systems for video technology*, 13(7):620–636, 2003. **1**
- [28] Fabian Mentzer, Eirikur Agustsson, Michael Tschannen, Radu Timofte, and Luc Van Gool. Conditional probability

- models for deep image compression. In *Proceedings of the IEEE Conference on Computer Vision and Pattern Recognition*, pages 4394–4402, 2018. 1
- [29] Fabian Mentzer, George D Toderici, Michael Tschannen, and Eirikur Agustsson. High-fidelity generative image compression. In H. Larochelle, M. Ranzato, R. Hadsell, M. F. Balcan, and H. Lin, editors, *Advances in Neural Information Processing Systems*, volume 33, pages 11913–11924. Curran Associates, Inc., 2020. 1, 2
- [30] David Minnen, Johannes Ballé, and George D Toderici. Joint autoregressive and hierarchical priors for learned image compression. In *Advances in Neural Information Processing Systems*, pages 10771–10780, 2018. 1, 2, 3, 5
- [31] Majid Rabbani. Jpeg2000: Image compression fundamentals, standards and practice. *Journal of Electronic Imaging*, 11(2):286, 2002. 1
- [32] Oren Rippel and Lubomir Bourdev. Real-time adaptive image compression. In *Proceedings of the 34th International Conference on Machine Learning-Volume 70*, pages 2922–2930. JMLR. org, 2017. 1
- [33] John Schulman, Philipp Moritz, Sergey Levine, Michael Jordan, and Pieter Abbeel. High-dimensional continuous control using generalized advantage estimation. In *Proceedings of the International Conference on Learning Representations (ICLR)*, 2016. 5
- [34] John Schulman, Filip Wolski, Prafulla Dhariwal, Alec Radford, and Oleg Klimov. Proximal policy optimization algorithms. *arXiv preprint arXiv:1707.06347*, 2017. 4
- [35] Hamid R Sheikh and Alan C Bovik. Image information and visual quality. *IEEE Transactions on image processing*, 15(2):430–444, 2006. 2
- [36] George Toderici, Damien Vincent, Nick Johnston, Sung Jin Hwang, David Minnen, Joel Shor, and Michele Covell. Full resolution image compression with recurrent neural networks. In *Proceedings of the IEEE Conference on Computer Vision and Pattern Recognition*, pages 5306–5314, 2017. 1
- [37] Aaron van den Oord, Nal Kalchbrenner, Lasse Espeholt, koray kavukcuoglu, Oriol Vinyals, and Alex Graves. Conditional image generation with pixelcnn decoders. In D. Lee, M. Sugiyama, U. Luxburg, I. Guyon, and R. Garnett, editors, *Advances in Neural Information Processing Systems*, volume 29. Curran Associates, Inc., 2016. 2
- [38] Xiaobo Wang, Shuo Wang, Cheng Chi, Shifeng Zhang, and Tao Mei. Loss function search for face recognition. In *International Conference on Machine Learning*, pages 10029–10038. PMLR, 2020. 2
- [39] Zhou Wang, Eero P Simoncelli, and Alan C Bovik. Multi-scale structural similarity for image quality assessment. In *The Thirty-Seventh Asilomar Conference on Signals, Systems & Computers, 2003*, volume 2, pages 1398–1402. Ieee, 2003. 1
- [40] Ronald J Williams. Simple statistical gradient-following algorithms for connectionist reinforcement learning. *Machine learning*, 8(3-4):229–256, 1992. 2, 4
- [41] Gengwei Zhang, Yiming Gao, Hang Xu, Hao Zhang, Zhen-guo Li, and Xiaodan Liang. Ada-segment: Automated multi-loss adaptation for panoptic segmentation. *arXiv preprint arXiv:2012.03603*, 2020. 2
- [42] Lei Zhou, Chunlei Cai, Yue Gao, Sanbao Su, and Junmin Wu. Variational autoencoder for low bit-rate image compression. In *CVPR Workshops*, pages 2617–2620, 2018. 1, 2, 5
- [43] Lei Zhou, Zhenhong Sun, Xiangji Wu, and Junmin Wu. End-to-end optimized image compression with attention mechanism. In *Proceedings of the IEEE Conference on Computer Vision and Pattern Recognition Workshops*, pages 0–0, 2019. 1, 2, 5